Tampere University

Henri Salonen

LABORATORY CHARACTERIZATION OF AUTOMOTIVE NIMH-BATTERY CELLS

Faculty of Information Technology and Communication Sciences
Bachelor's Thesis
April 2019

ABSTRACT

Henri Salonen: Laboratory Characterization of Automotive NiMH-Battery Cells
Bachelor's Thesis
Tampere University
Electrical Engineering
April 2019

This thesis was made to reflect on the measurements made on 10 battery modules of a total number of 28 modules from a Toyota Auris hybrid electric vehicle's battery system. The objective of the measurements was to ascertain the approximate values of capacity, efficiency and its dependency on the discharge current for each of the battery modules, and averages of the values of all of the battery modules.

The measurements were made as three separate charge-discharge-cycles for each of the 10 modules while measuring the voltage at the terminals of the battery module and the current to and from the battery module. The charging was done with a charging current of 2 A and the discharges with a constant discharge current of 5.0 A, 7.5 A and 10.0 A, respectively. The charging and discharging energy of each of the batteries was then calculated using the trapezoidal rule from the resultant voltage-current curves. The efficiency of each of the batteries was then calculated from comparing the discharging energy to the charging energy of each of the pairs.

The average capacity was calculated as approximately 29.7 W h, and the average efficiency was calculated as approximately 82.5%. The approximate total capacity of the battery system with 28 total modules was calculated as approximately 830 W h which is approximately 63.8% of the reference capacity. The dependency of efficiency from the discharge current was approximated with a fitted curve following the function $\eta = (-0.0024 \pm 0.0106)I_d + 0.83 \pm 0.0828$.

Keywords: battery, nickel-metal hydride, automotive, electric vehicle, hybrid

The originality of this thesis has been checked using the Turnitin OriginalityCheck service.

TIIVISTELMÄ

Henri Salonen: Sähköauton NiMH-akkukennojen laboratoriokarakterisointi
Kandidaatintyö
Tampereen yliopisto
Sähkötekniikka
Huhtikuu 2019

Tässä kandidaatintyössä tehtiin mittauksia Toyota Auris -hybridiauton akkumoduuleille. Mittaustuloksista määritettiin akkumoduulien kapasiteetti, akkumoduulin hyötysuhde ja sen purkuvirtariippuvuus, sekä koko akkujärjestelmän keskimääräinen kapasiteetti ja hyötysuhde. Näitä arvoja verrattiin edelleen referenssiarvoihin kirjallisuudesta.

Alkuperäisistä 28:sta akkumoduulista käytössä oli 10, joiden jännitettä ja virtaa mitattiin 3:lla erillisellä lataus-purku -syklillä. Latausvirta kaikissa sykleissä oli 2 A ja purku tehtiin vakiovirralla 5.0 A, 7.5 A, sekä 10.0 A, yksi mittaus jokaisella virralla. Mittauksista saadusta virta-jännitekäyrästä laskettiin likiarvo latausenergialle ja purkuenergialle puolisuunnikassäännön mukaisesti. Näistä arvoista laskettiin akkumoduulien hyötysuhde jakamalla purkuenergia saman syklin latausenergialla.

Keskimääräiseksi akkumodulin kapasiteetiksi saatiin laskennallisesti likimain 29.7 W h ja keskimääräiseksi hyötysuhteeksi likimain 82.5%. Keskimääräisestä kapasiteetista saatiin laskettua koko akkujärjestelmälle kapasiteetiksi likimäärin 830 W h, joka on noin 63.8% referenssiarvoon verrattuna. Hyötysuhteen riippuvuutta purkuvirrasta arvioitiin sovittamalla mittausdataan suora, jonka funktioksi saatiin $\eta = (-0.0024 \pm 0.0106)I_d + 0.83 \pm 0.0828$.

Avainsanat: akku, sähköauto, nikkeli-metallihydridi, hybridi

CONTENTS

LIST OF SYMBOLS AND ABBREVIATIONS

$\mathbf{E}$	energy
$\mathbf{I}$	current
$\mathbf{R}$	resistance
$\mathbf{Z}$	impedance
η	efficiency
BEV	battery electric vehicle
DC	direct current
EV	electric vehicle
HEV	hybrid electric vehicle
ICE	internal combustion engine
Li-ion	lithium-ion
NiMH	nickel-metal hydride
PHEV	plug-in hybrid electric vehicle
redox	reduction-oxidation reaction

1 INTRODUCTION

Cars and other motorized vehicles have been a mainstay of all transportation for well over a century. There were approximately 257 million personal cars in use in the European union in 2016 and as fossil fuels become sparser, it is imperative to investigate other energy sources [4]. One of the possibilities of these alternative propulsion methods is electricity.

Electric vehicles (EVs) are rapidly becoming more viable and popular as a means of transportation, as the combined total of passenger cars of battery electric vehicle (BEV) and plug-in hybrid electric vehicle (PHEV)-type reaching 1.2 million in Europe in 2018, compared to the around ten thousand in use in 2011 [3]. All electric vehicles need a battery system to store electrical power for their electric engine to use. Newer vehicle models use primarily lithium-ion (Li-ion) batteries for this purpose, but most of the earlier hybrid vehicles, excluding PHEVs, were designed to use nickel-metal hydride (NiMH) batteries which are still in regular use, but ageing.

In addition to vehicle applications, NiMH-battery technology is still in use in rechargeable batteries for electric appliances used by consumers everywhere, ranging from older laptop batteries to rechargeable AA and AAA -batteries. They replaced most of the earlier nickel-cadmium ones, and with their high tolerance for overcharge and -discharge it is practical to use them in applications where Li-ion ones are not stable enough. Military applications, for example, value NiMH-batteries for the increased reliability and stability that they provide.

This thesis is made to reflect on measurements made on ten battery modules of a Toyota Auris hybrid car. The measurement of the efficiency in the batteries gives an insight into the ageing of batteries in regular use in electric vehicles and can serve as the base data for making a mathematical model of the NiMH-batteries. The goal of the thesis is to present the data collected from the measurements of the battery modules, calculate the efficiency and capacity of the battery modules, estimate the internal resistance of the battery modules, and to compare the data to sources of reference.

Chapter 2 covers the theory of the batteries themselves with a focus on NiMH-batteries and their differences comparing to other batteries, followed by a brief history of batteries and their types in automation applications. Chapter 3 details the chosen method of measurement as well as the actual measurement system and its composition. The measurement data is presented in section 3.3, while in section 3.4 sources of error and their

impact on the data is evaluated. The results of the analysis are presented in section 3.5, and Chapter 4 presents the conclusions on the observed data and the measurements as a whole.

2 THEORY OF BATTERIES

Batteries are chemical electrical energy storages. There are many different battery construction methods and chemistries, that vary by application in size, capacity and composition. The types of batteries covered here will be centred around automotive NiMH-batteries, with other battery types only mentioned in comparison to them.

2.1 Basic Structure of Batteries

Battery as a term covers both primary batteries and secondary batteries. Their operation and chemistry are not too different from one another, but unlike secondary batteries, primary batteries are not designed to be recharged. [8, Ch. 1.2] Primary batteries are not used in automotive applications and thus only secondary batteries will be covered. The term battery is not as straightforward, as a battery system can be as small as a single, cased cell operating as a battery, a module that is built of several connected cells, or even a battery system comprised of several battery modules linked together and used as a single power source.

Figure 2.1 shows the basic structure of a battery cell, as well as the electrochemical operation while discharging. The basic reaction in both charging and discharging batteries is a reduction-oxidation reaction, in short called a redox-reaction. In the case of discharging, the positive electrode is acting as the cathode and is reduced, while the negative electrode acts as the anode and is oxidized.

Both electrodes are in contact with a medium called an electrolyte which facilitates ion transfer from one electrode to the other. The electrolyte is usually a liquid. Between the electrodes there is a separator, designed to prevent electron movement through the electrolyte, but allowing ions to pass through it from one electrode to the other. As seen in Figure 2.1 the current flows through the outer path, providing power to the load connected in between the battery terminals. To balance the change in charge, ions move from one electrode to the other, through the porous separator. The type of ions depends on the materials used in the electrodes. When the battery is being recharged, the roles of the electrodes are reversed. [9, pp.36-38]

Batteries can be designed and built in a multitude of ways, depending heavily on the purpose of the battery in question. Usual structural geometries for batteries are button cells, cylindrical cells and prismatic cells, with other geometries being less utilized in general [9, p.31]. Of these usual geometries the most well-known are the button and cylindrical cells

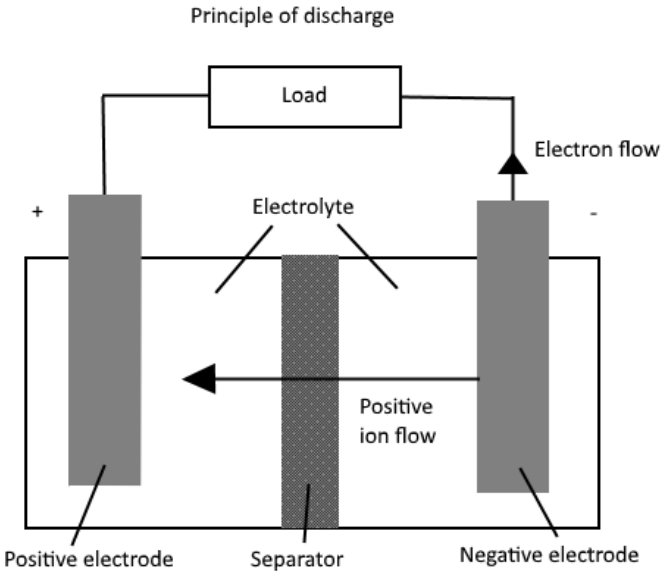

Figure 2.1. *The basic working principle of a discharging battery.*

which are used in electrical appliances found in most households. Automotive batteries often use a prismatic cell structure, usually a monobloc constructed battery module, consisting of several separate battery cells connected electrically to one another.

2.2 NiMH-battery Chemical Reactions

As discussed in 2.1, all batteries go through a redox-reaction in operation. The basic principle is the same for all batteries, but the materials used dictate the actual chemical process that takes place inside the cells. The characteristics of the materials used determine how the batteries perform under different conditions, and must be picked in accordance to the intended use of the battery. In addition, the actual structure of the battery changes the characteristics of a battery, affecting its performance and capacity.

NiMH-battery cells are composed of nickel oxyhydroxide (NiOOH) for the positive electrode, a metal hydride alloy for the negative electrode, and an electrolyte composed of usually around 30% potassium hydroxide (KOH) mixed in water [8, Ch. 22.3.4]. The composition of the metal hydride can vary very much, with three different compositions being listed in literature:

- AB_5 (LaCePrNdNiCoMnAl)
- AB_2 (VTiZrNiCrCoMnAlSn)
- A_2B_7 (LaCePrNdMgNiCoMnAlZr)

Of the listed compositions AB_5 is the most common, as its material costs are lower. These compositions may further vary in the amount of each element they are composed of. [8, ch. 22.3.2]

The chemical reaction for discharge in a NiMH-battery is a reduction-reaction from nickel oxyhydroxide to nickel hydroxide

$$NiOOH + H_2O + e \longrightarrow Ni(OH)_2 + OH^-$$

while the metal hydride (MH) is oxidized to a metal alloy (M)

$$MH + OH^- \longrightarrow M + H_2O + e$$

Combined, the equation of the two reactions is

$$MH + NiOOH \longrightarrow M + Ni(OH)_2$$

When the battery is being charged, the reaction is reversed. [8, Ch. 22.3.1]

As the battery is charged, the positive electrode reaches full charge before the negative one to prevent pressure buildup, as it starts to evolve oxygen, which travels to the negative electrode and reacts with the hydrogen to produce water.

The characteristics of NiMH-battery cells are presented in Table 2.1 with the values of both lead-acid and Li-ion batteries for comparison.

Table 2.1. *Characteristics of different chemistries in practical batteries. [8, Ch. 1.4.3]*

Chemistry	Cell voltage (V)	Specific energy ($W\,h\,kg^{-1}$)	Energy density ($W\,h\,l^{-1}$)
NiMH	1.2	100	235
Lead-acid	2.0	35	70
Li-ion	3.8	200	570

The values are of practical applications, while the theoretic values are slightly higher for each of the batteries. While NiMH-battery cells are superior in comparison to lead-acid ones in their specific energy as well as energy density, they clearly lose in this perspective to Li-ion.

2.3 Automotive Batteries

Batteries have been a part of the automotive technology for most of its lifetime. The definite first electric vehicle is up for debate, but all the candidates are from the end of the 19^{th} Century. In 1912 the electric starter was invented, and due to this, most cars to date have a battery in them. This development in internal combustion engine (ICE) vehicles in the early 20^{th} Century lowered the demand for electric vehicles, most probably due to the very low energy-to-weight ratio of the early batteries when compared to the gasoline used to power ICE vehicles.

2.3.1 History of Automotive Batteries and Battery Types

Early EVs were relatively popular at the turn of the 19^{th} Century. The batteries used in the earliest EVs were early lead-acid batteries, with an open design that had to be maintained much more than modern batteries. The batteries were heavy, and the range of the vehicles was limited to around 50 kilometers, but as cities were smaller and the road network outside them was not yet developed to suit the vehicles, the early electric vehicles were relatively widespread in their use.

As gasoline-powered, mass-produced ICE cars became a cheaper alternative, and the road networks developed enough to encourage the desire to drive cars for longer ranges, the early electric cars were no longer produced or bought. The development of electric cars ceased for a few decades, although the battery technology kept improving. In the 1970s lead-acid batteries were further developed to be sealed and maintenance-free and they are prominently used as ignition batteries in modern ICE cars to date. Military and scientific applications drove the development of batteries even further.

The oil crises in 1973, -79 and the 2000s prompted a more prominent development of alternative fuel source vehicles, since it was realized that gasoline was a finite resource, even if the shortages proved to be temporary. EVs and HEVs saw a new resurgence in development, with a few concept models being developed in the 1970s using lithium-nickel and nickel-cadmium -batteries. This resurgence culminated when Toyota introduced the first mass-produced HEV car, the Toyota Prius, in Japan in 1997. The Prius utilized a NiMH-battery to provide regenerative braking and electric launch to improve the fuel efficiency of the car [8, Ch. 29.5.1]. Alongside the NiMH-battery technology, Li-ion batteries were developed, and in 2008 the Tesla Roadster was introduced and it operated on Li-ion batteries [8, Ch. 29.1.1].

2.3.2 Use of NiMH-batteries in Automotive Applications

In automotive applications NiMH-batteries have mostly been in use in different types of hybrid vehicles. Hybrid vehicles come in different subtypes, namely in micro hybrids, mild hybrids, full hybrids and plug-in hybrids. They are categorized mostly by the capabilities of the electrical engine. Full hybrids have a limited capability of providing propulsion using just the electrical drive system, while mild hybrids can only support the ICE while it is in operation, and micro hybrids are used only so the ICE can be shut down while stopping briefly. Plug-in hybrids are further able to charge their batteries from external power sources. [8, Ch. 22.7.1]

In addition, the configuration of the drivetrain affects the usage of the battery. The configuration of the drivetrain can be a series, parallel or series-parallel drivetrain. In a series drivetrain the ICE is used to power a generator to recharge the batteries in drive and the electric engine is used for propulsion. This means the battery cycles constantly while in drive, effectively shortening the lifespan of the battery. In parallel configuration the ICE

and electric engine can both provide propulsion, as they are both connected to the transmission individually. This results in less use and wear for the battery. A series-parallel configuration is a combination of the two others. Both of the engines can provide propulsion independently, but the ICE is also used to drive a generator to recharge the batteries while in drive. [8, Ch. 29.5]

Table 2.2 shows the statistics compiled from available data of EVs by type in Europe and the United States in 2014 as well as the latest available statistics for each of them.

Table 2.2. *Cumulative number of EVs by type in 1000s of vehicles, compiled from [3], [5] and [4] for Europe, and from [2, p.137, 140–141] for the United States*

Vehicle type	EU, 2014	EU, 2018	US, 2014	US, 2016
HEV	-	2290	3536	4267
PHEV	71	629	150	266
BEV	123	637	136	295
Total	194	3556	3822	4828

The statistics for hybrids in Europe were unavailable for 2014. Considering that up until 2014 the Prius hybrid models have primarily used NiMH-batteries, with the PHEV model of Prius utilizing Li-ion batteries in 2013. Therefore, most of the early 2000s HEV and PHEV models were based on NiMH battery technology, then the amount of vehicles utilizing NiMH-batteries is probably at least several hundreds of thousands in Europe alone [11][12].

3 MEASUREMENT SYSTEM

The subject of the measurements were batteries from a Toyota Auris HEV that had been in regular use for 2 years. In this case the measurements for the battery characteristics were implemented using a charge-discharge cycle performed three times for each of the batteries at different discharge currents.

3.1 Measurement Method

Practical measurements have a multitude of parameters that affect the way they are set up, since there usually are many ways to do a certain measurement. The purpose of the measurements was to approximate the internal resistance of the battery, as well as calculate the efficiency of the battery in different charge-discharge cycles. Both of these could be obtained with the same measurement, as an unknown resistance is measured by supplying a known direct current to it, while measuring the voltage over it.

The simplest way to achieve this would have been to use two-wire sensing technique, but this would have left the resistance of the leads into the calculation, most probably causing a large calculation error [1, Ch. 13.6.2]. To eliminate the lead resistances from the measurement, a four-wire sensing technique was applied. The principle scheme of the measurement is shown in Figure 3.1.

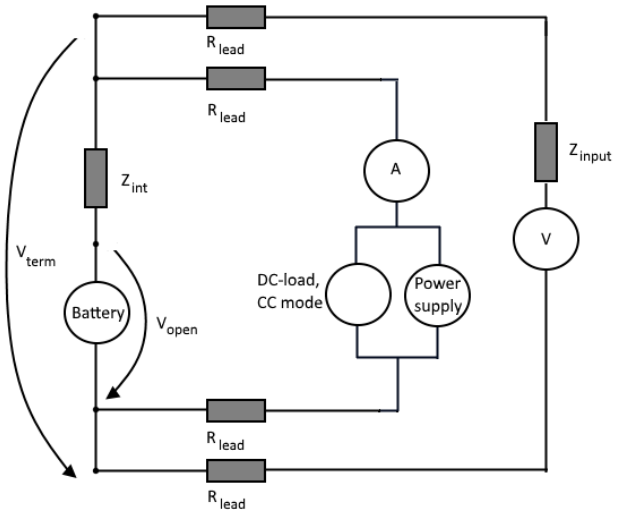

Figure 3.1. *The principal scheme of the measurement system.*

In this figure V_{open} is the open-circuit voltage of the battery, Z_{int} is the internal DC-resistance of the battery, R_{lead} is the resistance of the leads, Z_{input} is the input impedance of the oscilloscope, and V_{term} is the voltage from the battery terminals, which differs from V_{open} when there is a current to or from the battery. As the input impedance of the oscilloscope, acting here as the voltmeter, is 1 MΩ and is very large compared to the other impedances in the circuit, practically no current flows through the leads leading to it, thus reducing the effect of the lead resistance on the measured voltage to a minimum [1, Ch. 13.6.3]. Both the DC electronic load and the power supply were constantly connected to the circuit, even when the cycle was not using one of them.

Since the battery modules include six cells connected to each other, it was necessary to charge the batteries to a full charge, so the internal resistance and the efficiency would represent the whole module. The typical voltage curve during discharge for a fully charged prismatic sealed NiMH-battery cell is characterized by a sharp drop in voltage at the start of the discharge due to the internal resistance of the cell, after which the voltage curve stabilizes to a more gradual slope until the battery cell is mostly empty [8, Ch. 22.10.2]. While this is true for a single cell, a module consisting of multiple cells follows a similar curve. Continued discharge when the battery module is nearly empty results in a stepped curve, as the cells will reverse polarity one by one. This process usually renders the cells inoperable, thus ruining the battery module. Figure 3.2 shows an actual measurement that discharged the battery module for too long.

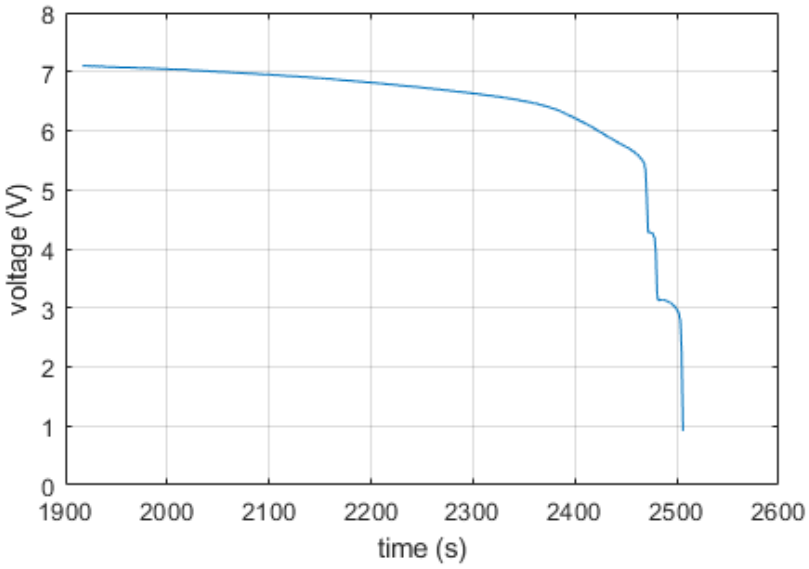

Figure 3.2. *The end of the discharge measurement zoomed to show the stepped curve*

Figure 3.2 is not the whole measurement, but a snapshot of the end of the measurement cycle to illustrate more clearly how a deep discharge affects a battery module. The start of the figure is from approximately 30 minutes into the measurement. As is evident from the curve, the cells start to reverse their polarity very soon after the terminal voltage of the battery drops below 6.0 V. The cut-off voltage had been approximated to be around 6.0 V according to the discharge curves found in literature, and the discharge in Figure 3.2

proved the cut-off to be accurate. There was no available way to control the DC electronic load in order to automate the cut-off at a certain voltage which would have alleviated the possible problem of overdischarge. With higher discharge currents the rate of voltage drop was also more rapid, and greater care was needed to cut the discharge before the voltage dropped too low.

Since the batteries in question had no given reference values, the recharge method had to be empirically tested to find a consistent state of charge to be used for all the battery modules in the test. Of the test subjects, battery modules $A18$, $A19$ and $A20$ were used to find the desired method of charging. The baseline for charging was set at around 7.5 V for the desired battery terminal voltage, as it is a typical operating voltage in such battery modules. After a few measurements using the baseline, the battery modules were observed to have a curve unlike the one expected from literature. At 2.0 A charging current, the voltage of the battery module rises too rapidly for it to reach full charge at the set baseline voltage. The voltage curves of the discharges at varied voltage targets are displayed in Figure 3.3.

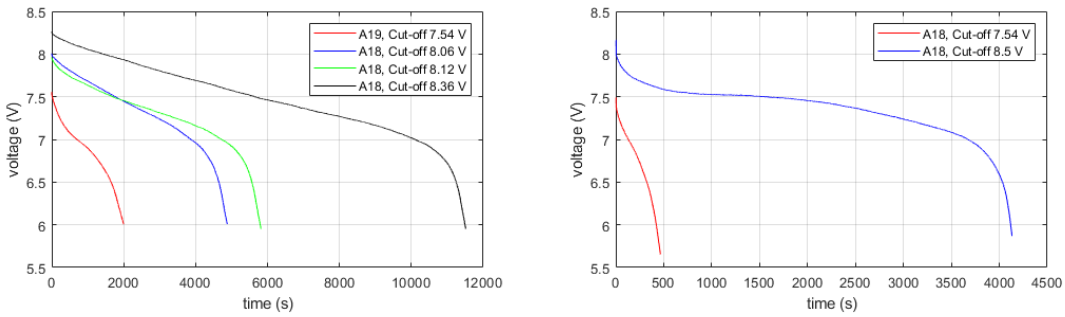

Figure 3.3. *Voltage curves from battery charging tests, discharge current for the tests in the left figure was 1 A and 5 A for the right.*

As can be seen from the figures, the slope of the voltage curve became more gradual and the steeper drop in voltage happened later in the curve as the batteries were charged to a higher voltage. Slower charging currents were experimented upon, but did not provide any better results, and would have resulted in even longer charging times. The resulting curve from a cut-off voltage of 8.5 V was one that resembled that of a normal discharge curve in literature and thus was determined to be the voltage to be used as cut-off for the charging. The time needed for the recharge is at least in part probably due to the speed of the chemical reactions inside the individual cells requiring time to settle. With a charging current of 2.0 A the charging of a battery module took approximately 3 hours. Higher charging currents would have been experimented upon, but the power supply could not provide more than the 2.0 A used.

3.2 Measurement Setup

As discussed in 3.1, the oscilloscope is set up to measure the voltage of the battery modules terminals and the current to and from the battery module using a current probe.

The physical setup is shown in Figure 3.4.

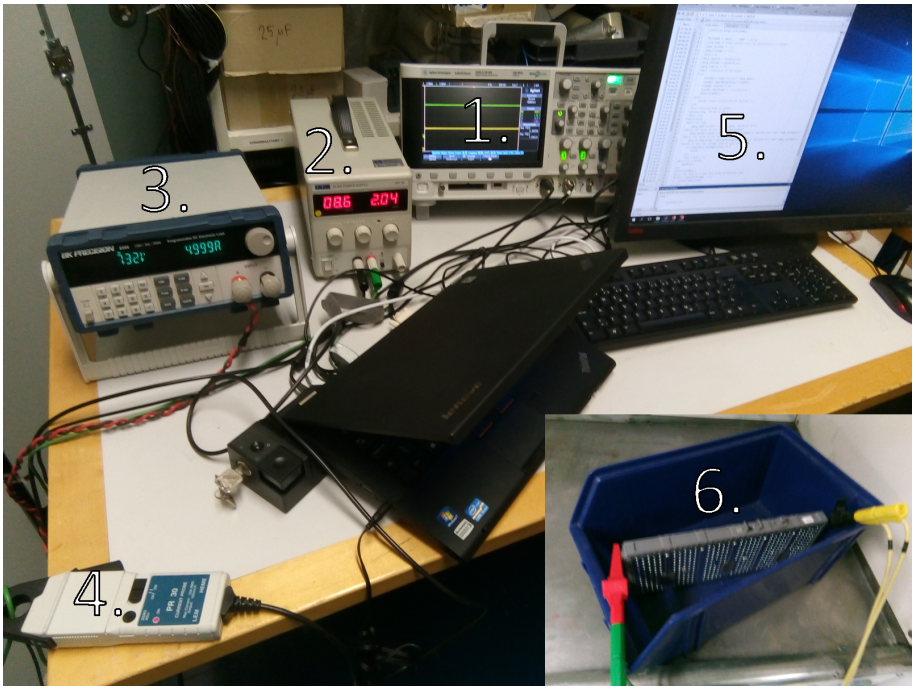

Figure 3.4. *The measurement setup pictured.*

The enumerated parts of Figure 3.4 are as follows:

1. Oscilloscope (DSO-X 2014A)
2. Power supply (EL302)
3. DC electronic load (BK Precision 8500)
4. Current probe (PR30)
5. Computer with MATLAB-script for control
6. The battery module

Referring to Figure 3.1, the oscilloscope measures V_{term} directly and reads the signal from the current probe, measuring the current to and from the battery. Both the DC electronic load and the power supply are connected to the wire passing through the current probe, with a discharging current from battery to load being marked positive. The voltage and current data were extracted from the oscilloscope at approximately 1 s intervals, recording the exact time and an average value for both the voltage and the current from the past second. These values were then recorded by the MATLAB-script to a file for further analysis.

The cycle was measured three times for each of the batteries. The charging current was set to 2.0 A, from which it would decline automatically once the terminal voltage approached the targeted full charge voltage of 8.50 V, since the power supply limits the current as it reaches the set voltage. The DC load was set to draw a discharge current at a constant rate of 5.0 A, 7.5 A and 10.0 A for each of the cycles, respectively. The

charging of a single battery module took roughly 3 hours, which meant that the time between charge and discharge could not reasonably be kept constant.

3.3 Measurement Results

To estimate the amount of energy charged and discharged in each cycle, the power of a measurement point was calculated by multiplying the current with the voltage of the given measurement point. The resulting power-time curve was then integrated using the trapezoidal method, in which the area of the curve is numerically integrated assuming a linear change between two measurement points, resulting in an area consisting of trapezoids for easier calculation. The efficiency of the discharge is then calculated with the formula $\eta = \frac{E_d}{E_c}$. All of the calculated values for the measurement cycles can be found in the Appendix A.

Table 3.1 shows the averaged values of energy discharge and efficiency per module and for all the battery modules in total. Values deemed as errors have been omitted from the calculations.

Table 3.1. *Averages of energy discharge and efficiency per module and in total*

Module	Avg. E_d (W h)	Avg. η
A18	43.456	0.818
A19	42.163	0.793
A21	28.247	0.799
A22	28.896	0.814
A23	23.982	0.792
A24	22.743	0.788
A25	26.126	0.930
A26	25.028	0.901
A27	26.874	0.786
A28	29.227	0.832
Total	29.674	0.825

The values of the individual battery modules are mostly similar for both the capacity and efficiency. The reference for a NiMH-battery's efficiency in literature is high, even over 90 % [8, Ch. 22.10.10]. Compared to it, the efficiencies of the individual modules are somewhat lower, but seem plausible considering the use the battery modules have seen.

3.4 Evaluation of Errors

As with any actual measurement, there are always some errors. It is imperative to evaluate the nature of the possible errors to better evaluate the validity of the data acquired in the measurements. Errors in this case can be categorized into instrumental accuracy and errors in the setup.

Instrumental errors are in this specific case limited to the inaccuracies of the oscilloscope and the current probe connected to it, while the accuracy of the power supply and the DC electronic load do not matter. The gain error of the oscilloscope for the settings used was $\pm 0.522\,\mathrm{V}$, but this error is static and could be compensated, while the error from noise is very small compared to the measured voltages [6, p.15]. The current probe inaccuracy is dependent on the current measured and thus was at most $\pm 0.102\,\mathrm{A}$ for the 10.0 A measurements [7].

The measurements could have been improved by having the cut-off limits enforced automatically by the measurement devices. This would have eliminated the human factor in evaluating the time of cut-off which would have resulted in more consistent charge and discharge cycles. This was not possible due to the equipment used in the measurement. If the shield values of the batteries being tested were known, the proper procedure for charging them would have been more defined, possibly resulting in a better performance by the batteries in the measurements. It would have also ensured that the battery modules got charged to their maximum capacity at each charge cycle. Unfortunately the values were not available for use. For more consistency, the measurement of the charge and discharge could have been made with a set time between them, especially if the power source and the DC electronic load could have been controlled. The discharge measurements were mostly made immediately after the measurement of the charge was done, but in some cases the battery modules had to be left disconnected overnight. Whether the time between the measurements had any impact was left undetermined.

Furthermore, having more measurements per battery module of the same discharge current would have resulted in more data to compare, allowing for a more accurate evaluation of the accuracy and consistency of the measurement. Additional values of discharge currents would have provided a more broad set of data to analyse. Since it was possible to measure only one battery module at a time, the long charge time of the battery modules would have made additional measurements impossible in the time frame of the project.

3.5 Results of Analysis

With the average energy discharged at 29.7 W h, the total capacity of the battery system of 28 battery modules can be approximated to be around 830 W h. An approximate reference value for the battery system could be derived from the electric charge in A h multiplied by the voltage of the whole battery system for a total of approximately 1300 W h [10, p.496]. In its current state, the battery system can hold approximately 63.8% of its original capacity. The decrease in capacity seems large, considering the average lifetime of a vehicle, and that the vehicle had been in use for only two years, but there were no actual reference values available to compare to.

Figure 3.5 shows the efficiency values by discharge current. Each of the marker-color pairs represents the measurement data for a specific battery module. The curve of the fit is also represented on the figure.

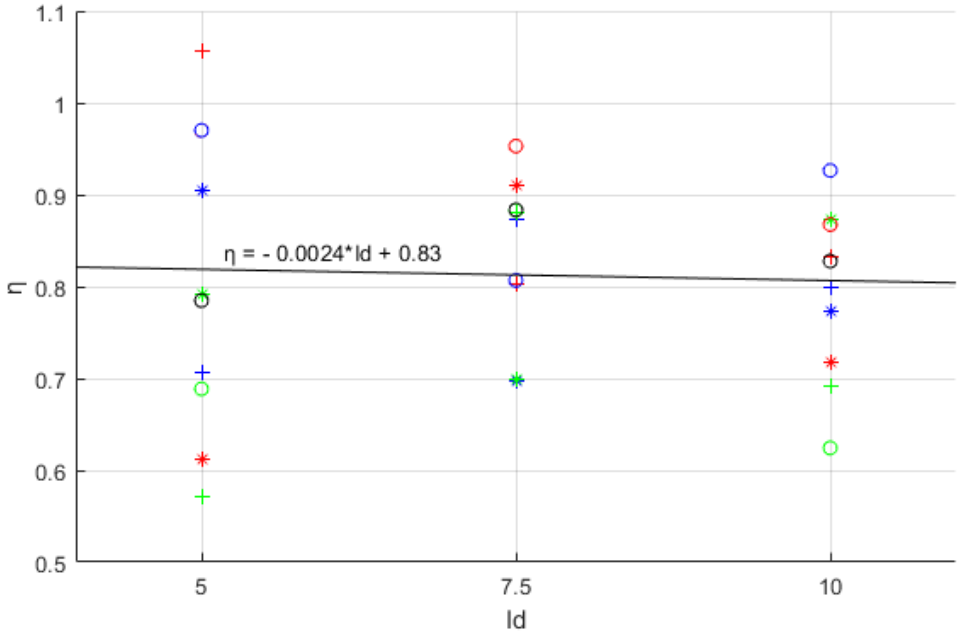

Figure 3.5. *Efficiencies of each of the measurements by discharge current.*

The efficiency values for the measurements made at $I_d = 5.0\,\mathrm{A}$ show a large dispersal, but overall the data shows a probable linear correlation between the η and I_d in this range. Calculations of a linear fit model to the data resulted in a fit following the curve $\eta = (-0.0024 \pm 0.0106)I_d + 0.83 \pm 0.0828$ accounting for standard error. Considering that in literature the efficiency of the batteries drops the more current is drawn from them, this curve seems plausible, but the positive coefficient values resulting from the standard error should probably be ignored. The large dispersal in the data shows a correlation, but more data should be gathered before a model of reasonable accuracy can be formed.

4 CONCLUSIONS

The objective of the thesis was to evaluate the characteristics of the NiMH-battery cells after two years of active use compared to the values found in literature. To gauge the characteristics of the battery modules each of the battery modules was measured with three separate charge-discharge cycles. The measurements made were successful and provided mostly plausible values for the characteristics. An average capacity of 29.7 W h was calculated for the battery modules with an average efficiency of 82.5%. The whole battery system was approximated to have a capacity of 830 W h. It is approximately 63.8% compared to the reference values of the battery system. Efficiency of the battery modules was approximated to be dependent from the discharge current along a curve following the function $\eta = (-0.0024 \pm 0.0106)I_d + 0.83 \pm 0.0828$.

The average efficiency is within expected limits, as NiMH-batteries have a high efficiency in general. The total capacity of the battery system is approximately a third lower compared to the reference value, which is an unexpectedly large drop for only two years of use. The battery system cycles consistently in a series-parallel hybrid drivetrain, but the expected lifetime of the batteries is generally longer. The seemingly low capacity measured could also be an indication that the battery modules were charged or discharged in an unoptimized way which is certainly possible, as there were no official operating procedures to refer to. The data gathered has a lot of dispersion and additional measurements would have provided a more accurate representation of the properties of the battery modules. Further study is needed to provide consistent data to form a working model of the battery modules.

REFERENCES

[1] C. F. Coombs, B. Stahlin, D. R. Workman, F. Cruger, J. F. Dias, J. J. Corcoran, C. Kingsford-Smith, W. Heinz, J. Guilford, T. Mikkelsen, J. S. Gallo, J. Ryles, S. Stever, A. J. De Vilbiss, R. E. Pratt, A. Pfaff, R. Chappell, L. S. Cutler, J. A. Kusters, A. W. Schmidt, W. Ishak, Y. Narimatsu, J. L. Hook, D. R. Harkins, S. Warntjes, S. Witt, H. Walker, F. K. David, K. D. Baker, D. A. Burt, J. M. McGillivary, C. Erickson, D. Richey, P. Christ, T. Tillson, J. E. Mueller, D. Kwock, G. Georg, and K. Lee. *Electronic instrument handbook*. English. 3rd. New York: McGraw-Hill, 2000. ISBN: 9780070126183.

[2] S. C. Davis, S. E. Williams, R. G. Boundy, and S. Moore. *2016 Vehicle Technologies Market Report*. Data available at .../vtmarketreport/technologies.shtml. 2017. URL: https://cta.ornl.gov/vtmarketreport/pdf/2016_vtmarketreport_full_doc.pdf (visited on 04/01/2019).

[3] European Alternative Fuels Observatory. *Total Number of Alternative Fuels Passenger Cars*. Filtered by electricity as the power source. Mar. 30, 2019. URL: https://www.eafo.eu/vehicles-and-fleet/m1 (visited on 03/30/2019).

[4] European Automobile Manufacturers' Association. *ACEA Report. Vehicles in use, Europe, 2018*. Nov. 11, 2018. URL: https://www.acea.be/uploads/statistic_documents/ACEA_Report_Vehicles_in_use-Europe_2018.pdf (visited on 04/14/2019).

[5] European Automobile Manufacturers' Association. *Passenger Car Registrations by Fuel Type*. Feb. 7, 2019. URL: https://www.acea.be/uploads/press_releases_files/20190207_PRPC_fuel_Q4_2018_FINAL.pdf (visited on 04/01/2019).

[6] Keysight. *InfiniiVision 2000 X-Series Oscilloscopes Data Sheet*. Apr. 20, 2019, 23. URL: http://literature.cdn.keysight.com/litweb/pdf/5990-6618EN.pdf (visited on 04/20/2019).

[7] LEM. *LEM PR 30 Current Probe Datasheet*. Apr. 5, 2019. URL: www2.elo.utfsm.cl/~elo382/wp-includes/images/PR30.pdf (visited on 04/05/2019).

[8] D. Linden, D. Linden, and T. B. Reddy. *Linden's Handbook of batteries*. eng. 4th ed. New York: McGraw-Hill, 2011, ca. 1200. ISBN: 978-0-07-162421-3. URL: https://tut.finna.fi/Record/tutcat.234472.

[9] A. Rautiainen, K. Vuorilehto, A. Supponen, J. Rekola, and J. Mäkinen. *Electrical Energy Storages and Electric Vehicles*. Lecture notes for course DEE-54206. 2018.

[10] Toyota. *Toyota Auris Owner Manual*. Mar. 1, 2016, 660. URL: https://d24bc9lyrt5en5.cloudfront.net/Customer-Portal-Admin/emanuals/TOYOTA/OM12J68FI_Auris+Hybrid_151207_INS_2C.pdf (visited on 04/12/2019).

[11] Toyota. *Toyota Prius 2013 Product Specifications*. Apr. 1, 2019. URL: https://toyotanews.pressroom.toyota.com/releases/2013+toyota+prius+product+specs.htm (visited on 04/01/2019).

[12] Toyota. *Toyota Prius Plug-In Hybrid 2013 Product Specifications*. Apr. 1, 2019. URL: https://toyotanews.pressroom.toyota.com/releases/2013+toyota+prius+plug+in+product+specs.htm (visited on 04/01/2019).

A CALCULATED ENERGY AND EFFICIENCY VALUES

Module, cycle	I_d (A)	E_c (W h)	E_d (W h)	η
A18,1	5.0	–43.015	45.416	1.056
A18,2	7.5	–55.068	44.189	0.802
A18,3	10.0	–51.300	42.723	0.833
A19,1	5.0	–63.902	45.099	0.706
A19,2	10.0	–50.666	40.516	0.800
A19,3	7.5	–46.861	40.875	0.872
A21,1	10.0	–37.261	25.802	0.692
A21,2	7.5	–34.862	30.692	0.880
A21,3	5.0	–36.648	20.963	0.572
A22,1	10.0	–40.708	29.222	0.718
A22,2	7.5	–31.362	28.570	0.911
A22,3	5.0	–30.446	18.632	0.612
A23,1	10.0	–31.016	23.982	0.773
A23,2	5.0	–31.127	28.185	0.905
A23,3	7.5	–28.788	20.069	0.697
A24,1	5.0	–28.720	22.743	0.792
A24,2	10.0	–28.642	24.992	0.873
A24,3	7.5	–27.601	19.304	0.699
A25,1	10.0	–30.116	26.126	0.868
A25,2	7.5	–26.564	25.315	0.953
A25,3	5.0	–26.236	25.450	0.970
A26,1	10.0	–27.017	25.028	0.926
A26,2	5.0	–27.804	26.974	0.970
A26,3	7.5	–29.516	23.814	0.807
A27,1	5.0	–37.458	25.795	0.689
A27,2	7.5	–31.654	27.953	0.883
A27,3	10.0	–33.603	20.980	0.624
A28,1	10.0	–36.566	30.266	0.828
A28,2	5.0	–34.075	26.743	0.785
A28,3	7.5	–34.715	30.673	0.884